Diagnostics of Atomic Oxygen in Arc-Heater Plumes

Makoto MATSUI*, Kimiya KOMURASAKI†,
and Yoshihiro ARAKAWA‡
University of Tokyo
7-3-1 Hongo, Bunkyo, Tokyo 113-8656, Japan
81-03-5841-6586
And
Masahito MIZUNO§
National Aerospace Laboratory of Japan (NAL)
7-44-1 Jindaiji Higashi-machi, Chofu, Tokyo, 182-8522, Japan
matsui@al.t.u-tokyo.ac.jp

IEPC-01-195

Absorption spectroscopy has been applied to the measurement of the arc-heater plumes. Number density and translational temperature of atomic oxygen were obtained from the measured absorption line profile at 777.19 nm. , In a nitrogen-oxygen plume at the total enthalpy of 19.3 MJ/kg, density distribution in the shock layer formed by the TPS material has been obtained. It was much smaller than theoretical estimation. The maximum density of oxygen was about 10^{16}[m^{-3}]. In an argon-oxygen plume at the total enthalpy of 6.1 MJ/kg, distributions of number density of atomic oxygen (~10^{17}[m^{-3}]) and translational temperature (~6,000[K]) were obtained. As a result, the oxygen injected at the constrictor is found gradually diffusing from the outer region toward the centerline in the plume, resulting in the unexpectedly low degree of dissociation.

Introduction

Arc-heaters/arcjets are used for the tests of Thermal Protection Systems for reentry vehicles and for propulsion in space. However exact plume conditions are mostly unknown because it is usually in thermo-chemical nonequilibrium. Therefore, measurement of chemical composition in the plume will provide useful information for TPS researches and thruster development, and also for validation of numerical codes for high-speed reacting gas flow simulation.

Recently, non-intrusive spectroscopy, especially emission one is actively done to examine the characteristic of such high temperature and high Mach number flows. [1], [2] As a result, excitation, vibration, and rotational temperatures of atoms and molecules in the flow are being clarified. However, it was difficult to measure a chemical composition of the flow, in a word, number density by emission spectroscopy.

The Laser Induced Fluorescence is one of the most powerful spectroscopy because it is able to get the atomic number density of the ground state directly. In addition, this method is sensitive and applicable to a low-density flow (~10^{8}[m^{-3}]). [3],[4] However it is not applicable to optically thick plasma due to strong spontaneous emission and reabsorption. Moreover, a huge, expensive laser such as excimers is needed to excite the ground state of atoms.

Diode-laser absorption spectroscopy has two

* Graduate Student, Department of Advanced Energy
† Associate Professor, Department of Advanced Energy
‡ Professor, Department of Aeronautics and Astronautics
§ Researcher, Fluid Science Research Center, at that time NASDA Research Fellow

major advantages. It is applicable even to optically thick flows and it does not require the absolute absorption quantity but the relative absorption one. Table 1 shows the comparison of these three non-intrusive spectroscopy methods.

Table 1. Comparison of three spectroscopes

	Absorption	Emission	LIF
Alignment	Easy	Difficult	Very difficult
Sensitivity	Low	High	High
Absolute calibration	No need	Absolute light source	Reference cell
Optically thick plasma	Possible	Impossible	Impossible
Spatial resolution	Poor	Good	Very good
Portability	Easy	Possible	Impossible

Number density of atomic oxygen in a plume is quite important for studies of surface catalysis and oxidization of TPS. Therefore, in this research the absorption spectroscopy has been conducted targeting the atomic oxygen. By modulating the laser wavelength around the absorption one, the absorption profile is obtained. Number density in a metastable state is obtained from its integrated absorption coefficient and translational temperature is obtained from its broadening. The Grotian diagram corresponding to this transition is shown in Fig1.

Measurement theory

In this research the absorption profile was measured for the transition of $3s5S2 \rightarrow 3p5P3$, which is a mtastable state of atomic oxygen at 777.19nm.

Absorption coefficient

The relationship between laser intensity I_ν and absorption coefficient k_ν in a substance is expressed by Beer-Lambert law as,

$$\frac{dI_\nu}{dx} = -k_\nu I_\nu \tag{1}$$

Equation (1) is integrated as,

$$\ln\frac{I_\nu}{I_{\nu 0}} = -\int k_\nu dx \tag{2}$$

Here, $I_{\nu 0}$ I_ν, ν are incident laser intensity, transmitted laser intensity, laser frequency, respectively. Assuming the axisymmetric distribution, eq.(2) is expressed as,[5]

$$\ln\frac{I_\nu}{I_{\nu 0}}(y) = -2\int_y^{\sqrt{r^2-y^2}} \frac{k_\nu(r)\cdot r}{\sqrt{r^2-y^2}} dr \tag{3}$$

Equation (3) is inverted as,

$$k(r) = \frac{1}{\pi}\int_r^R \frac{d\left(\ln\frac{I_\nu}{I_{\nu 0}}(y)\right)}{dy}\frac{dy}{\sqrt{y^2-r^2}} \tag{4}$$

As a result, the absorption coefficient is obtained from the absorption ratio.

Since the local absorption coefficient is a sum of an absorption coefficient and a stimulated emission coefficient, the relationship between integrated absorption coefficient $K(r)$ and population density at the absorbing state n_i is given as[6],[7]

$$K(r) = \int k_\nu d\nu = \frac{\lambda^2}{8\pi}\frac{g_j}{g_i}A_{ji}n_i\left[1-\exp\left(-\frac{\Delta E_{ij}}{kT_{ex}}\right)\right] \tag{5}$$

Here, i, j are lower and upper energy levels, A_{ij} is the Einstein's transition probability, g_i and g_j are statistical weights, E, k and T_{ex} are energy level, Boltzmann constant and electronic excitation temperature, respectively. The transition data of atomic oxygen at 777.19nm is shown in Table 2.

Table 2. Transition data of atomic oxygen

i	j	λ(nm)	E_i(cm^{-1})	E_j (cm^{-1})	g_i	g_j	A_{ji}(10^8s^{-1})
3s5S	3p5P	777.19	73768.20	86631.45	5	7	0.369

At 777.19 nm, $\Delta E_{ij}/k$ is 18,500 K. If $T_{ex} \lesssim \Delta E_{ij}/k$, stimulated emission is neglected and Eq. (5) is simplified as

$$K = \frac{\lambda^2}{8\pi}\frac{g_j}{g_i}A_{ji}n_i \tag{6}$$

Absorption profile

Absorption profile is broadened by various physical mechanisms such as the thermal motions of surrounding particles and oneself, and is expressed by a convolution of the Lorentz-type and the Gauss-type distribution.

Doppler broadening

Doppler broadening is the statistical one originating from thermal motion of the particle and Gauss type.

$$\Delta\nu_D = \frac{\sqrt{8R\ln 2}}{\lambda_0}\sqrt{\frac{T}{M}} \tag{7}$$

Here, c is the velocity of light, R is the gas constant, λ_0 is the center frequency of the laser and M is the atomic weight of the absorbing atom. From this relationship, the translational temperature is obtained.

Other broadenings

Natural broadening is caused by the fact that there is finite time for the transition and expressed as,

$$\Delta\nu = \frac{A}{2\pi} \tag{8}$$

Pressure broadening is caused by collisions between atoms and particles around them and expressed as,

$$\Delta\nu_L = 1.95\times10^{13}\, p\sigma_L{}^2 \sqrt{\frac{2R}{\pi T}\left(\frac{1}{M_1}-\frac{1}{M_2}\right)} \tag{9}$$

Here, σ_L is effective collisional cross-section, p is the gas pressure, M_1 is atomic weight of absorbing atom, and M_2 is atomic weight of atmosphere gas.

Stark broadening originates from the fact that the degeneracy is solved by the electric field which a surrounding electron makes, and is expressed by as,[8]

$$\Delta\lambda_s = 2\left[1+1.75\times10^{-4} n_e^{1/4}\alpha\left(1-0.068 n_e^{1/6} T_e^{-1/2}\right)\right] n_e w\cdot10^{-16} \tag{10}$$

Here, w is electron impact parameter, α is the ion broadening parameter, n_e is electron density, T_e is electron temperature. These broadenings are all Lorenz type and three orders of magnitude smaller than that of Doppler broadening under our measurement conditions. Therefore, they are neglected.

The relationship between these physical parameters and absorption profiles are illustrated in Fig.2.

Experimental Apparatus

Optical system

Figure 3 shows the schematic of an optical system used in this research. A diode-laser with an external resonator (Velocity Model 6300) was used as the laser oscillation source. The line-width of the laser is smaller than 300kHz. The diameter of the probe laser beam is 2mm and the modulation frequency is 20 Hz. An optical isolator is used to prevent the reflected laser beam from returning into the external cavity. A Fabry-Perot, etalon, whose free spectral range is 1 GHz, is used as a wave meter. The laser beam was introduced into a vacuum chamber through an optical fiber.

Arc heater

The JUTEM arc-heater was used. It was developed for material tests in very high temperature environment. The schematic of the JUTEM arc-heater is shown in Fig.4. Oxygen is injected in the constrictor part in order to prevent the cathode from oxidization. The flow Mach number at the nozzle exit is designed at 3. A photograph of the arc-heater plume is shown in Figs.5 and 6.

Test conditions

Two cases were tested as listed in Table 3. The case No.1 is the measurement in a shock layer generated in front of a cylinder-shape SiC TPS material in a nitrogen-oxygen flow. This flow consists of 20 [slm] nitrogen and 5 [slm] oxygen. The input power is 21.6 kW and specific enthalpy in the centerline is estimated to be 19.3 MJ/kg from the measurement heat flux and pitot pressure.

The case No.2 is the measurement in the argon-oxygen free stream. This flow consists of 20 [slm] argon and 5 [slm] oxygen. The input power is 7.2 kW and specific enthalpy is estimated to be 6.1 MJ/kg assuming that thermal efficiency is 60%. In both cases, backpressure was kept at 38 [Pa].

Table 3. Experimental condition

No.	Gas flow	Specific enthalpy	Position
1	N_2: 20[slm] O_2: 5 [slm]	19.3 [MJ/kg] (On the centerline)	In the shock layer
2	Ar: 20[slm] O_2: 5[slm]	6.1 [MJ/kg] (Average)	In the free stream

Typical signals and a normalized absorption profile of atomic oxygen are shown in Figs.7 and 8.The profile is fitted by a Gauss function.

Result and Discussion

The number density distribution in case No.1 is shown in Fig.9. The distribution was different from our expectation on the following two points: 1) number density of atomic oxygen is much smaller than the estimation assuming fully dissociation; 2) the peaks of distribution were located off axis.

This result gave us a picture of the mixing process of nitrogen and oxygen shown as in Fig.10. Oxygen injected at the constrictor is not enough mixed with nitrogen in the nozzle. Then, it diffuses from outer to inside, with being dissociated in the free stream. Therefore, oxygen does not pass through the high temperature cathode jet region, resulting in low degree of dissociation.

To clarify this hypothesis, the measurement of atomic oxygen distribution in a free stream was conducted. Since absorption in a nitrogen-oxygen free stream is too small to measure, the argon-oxygen stream is tested instead of nitrogen-oxygen one, in which absorption is large enough to be detected.

Figures11 and 12 show translational temperature and number density distributions of atomic oxygen, respectively. The distribution of number density at z=100mm has peaks at r=20mm (z and r are defined by cylindrical coordinate and origin is taken at the

center of the nozzle exit). At z=150mm, these peaks approach to the centerline and combine at z=250mm. In contrast, the distribution of translational temperature at z=100mm has a peak on the centerline, and it separates into two peaks at z=150mm. The maximum number density and translational temperature are 3.1×10^{16}m^{-3} and 6200K, respectively.

From the measured thermo-chemical properties in the free stream, the oxygen mixing process can be explained as follows.

1) Previously, oxygen is not enough mixed with argon in the nozzle and diffusing from outer to inside in the free stream.
2) Steep temperature peak originated from the cathode jet is gradually relaxed by the dissociation of molecular oxygen.

Summary

1. Number density and translational temperature of the atomic oxygen were deduced from the measured absorption profile at 777.19nm by a diode absorption spectroscopy
2. The distributions of number density and tranlational temperature of atomic oxygen in the shock layer of nitrogen-oxygen flow and in the argon-oxygen free stream were obtained.
3. In the nitrogen-oxygen shock layer, number density of atomic oxygen was much smaller than the estimation assuming fully dissociation, and the peak of distribution was located off axis
4. In the argon-oxygen free stream, oxygen was found diffusing from outer to inside. Since, oxygen does not pass through the cathode jet region, in which temperature is very high, resulting in low degree of dissociation.

Acknowledgment

The authors thank NASDA for coordinating the experiment at JUTEM.

References

[1] Tahara, H. Taniguchi, T, Onoe, K, Yoshikawa, T .: DC Arcjet Plasma characteristics using ammonia and mixture of nitrogen and hydrogen, AIAA paper 99-3736, July, 1999.

[2] Winter, M. W. and Auweter-Kurtz, M.: Boundary layer investigation in front of a blunt body in a subsonic air plasma flow by emission spectroscopic means, AIAA paper 98-2460, June, 1998.

[3] Storm, P. V. and Cappelli, M. A.: Laser-induced fluorescence measurements within an arcjet thruser nozzle, AIAA paper 95-2381, July 1995.

[4] Feigl, M., Dennis, J. E., Fasoulas, S. and Auweter-Kurtz, M.: Comparison of LIF and solid electrolyte sensor measurements of atomic and molecular oxygen in a plasma jet, AIAA paper 2000-0198, January 2000.

[5] Deutch, M., Abel inversion with a simple analytic representation for experimental data, *Appl. Phys. Lett*., Vol 42, pp 237-239, 1983

[6] Zel'dovich, Y. B., Raizer, Y. P., Hayes, W. D. And Probstain, R. F.: *Physics of shock waves and high-temperature hydrodynamic phenomena*, Academic Press New York (1966), pp. 107-172.

[7] Lochte-Holtgreven W.: *Plasma Diagnostics*, Norty-Holland Publishing Company, Amsterdam (1968), pp. 9-65.

[8] Arroyo, M. P., Langlogis, S. and Hanson, R. K.: Diode-laser absorption technique for simultaneous measurement of multiple gasdynamic parameters in high-speed flows containing water vapor, *App. Opt.,* Vol. 33 (1994), pp.3296-3370.

[9] Komurasaki, K, Sugimine, M, Hosoda, S., and Arakawa, Y.: Laser Absorption Measurement of Atomic Oxygen in Arc-Heater Plumes, AIAA paper 2001-0814

[10] Bear, D. S., Chang, H. A. and Hanson, R. K.: Semiconductor laser absorption diagnostics of atomic oxygen for atmospheric-pressure plasmas, AIAA paper 98-0822, 1998.

[11] Griem, H., *Plasma Spectroscopy*, McGraw Hill, New York (1964)

[12] Herzberg, G., *Atomic spectra and atomic structure, Dover Publications*, New York (1944)

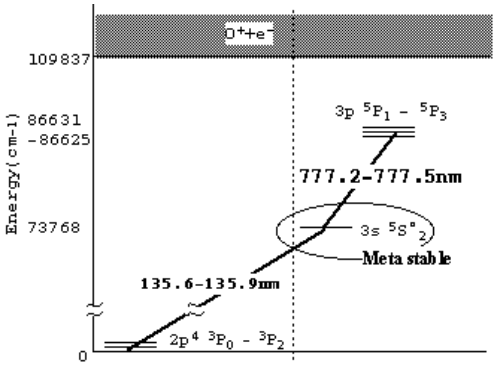

Fig.1 - Grotrian diagram of Oxygen

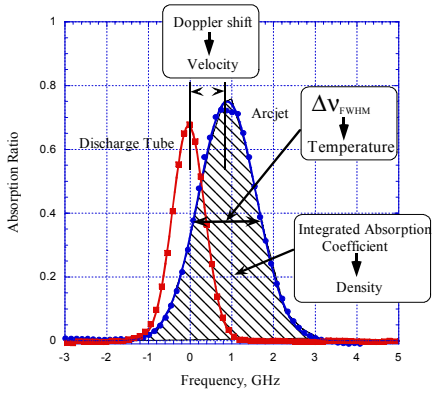

Fig.2 - Relationship between physical parameters and absorption profiles

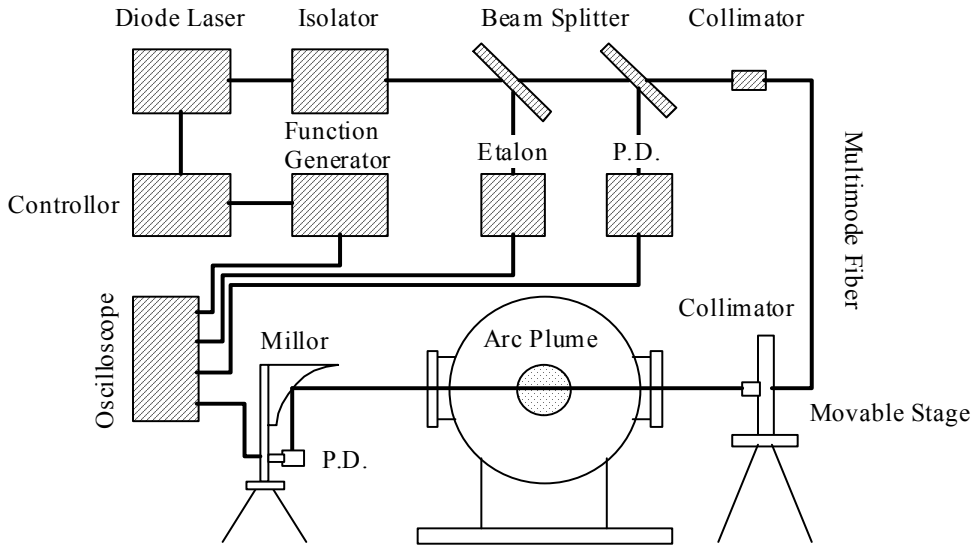

Fig.3 - Schematic of measurement system

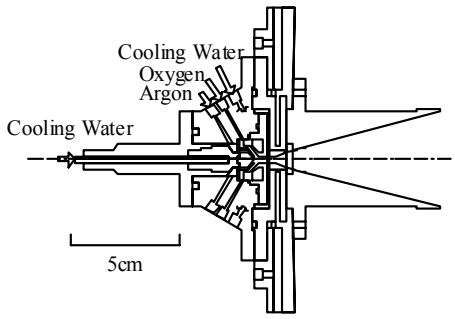

Fig.4 - JUTEM Arc-heater

Fig.5 - Nitrogen-oxygen plume

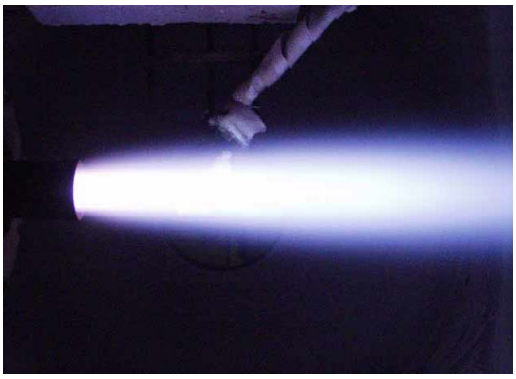

Fig.6 - Argon-oxygen plume

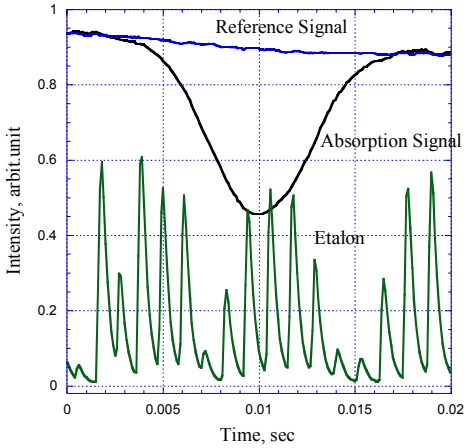

Fig.7 - Typical signals

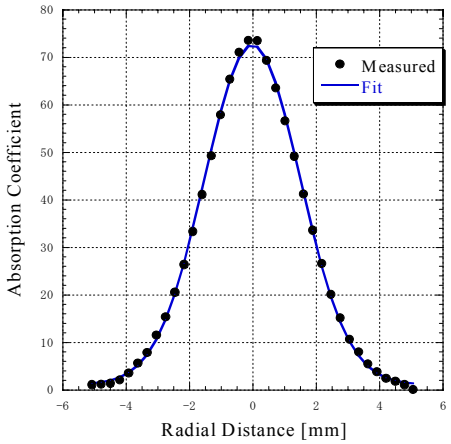

Fig.8 - Normalized absorption profile

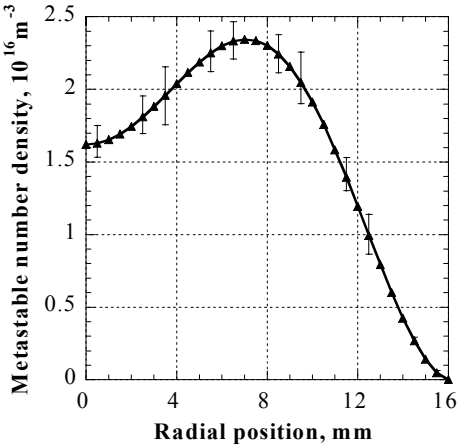

Fig.9 - Radial distribution of number density in nitrogen-oxygen shock flow

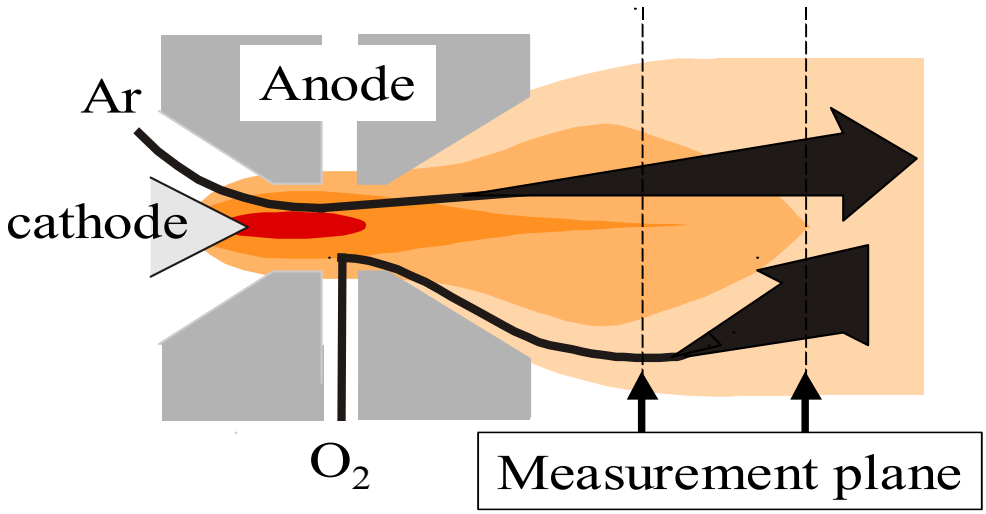

Fig.10 - Mixing process

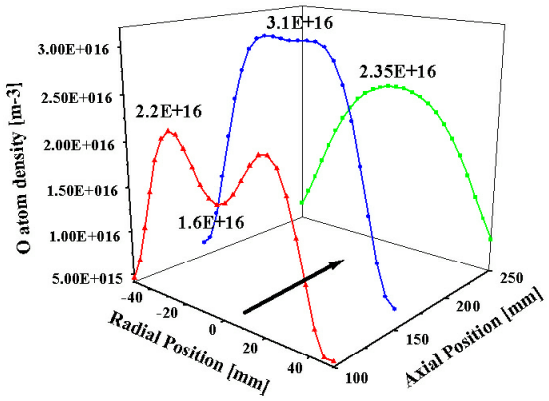

Fig. 11 - Number density distribution of atomic oxygen in argon-oxygen plume

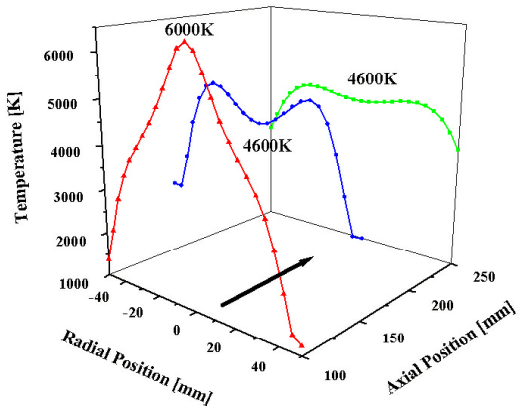

Fig.12 - Translational temperature distribution of atomic oxygen in argon-oxygen plume